THE JOURNAL OF BIOLOGICAL CHEMISTRY VOL. 281, NO. 23, pp. 15709–15713, June 9, 2006

SecA Supports a Constant Rate of Preprotein Translocation*[S]

Received for publication, January 9, 2006, and in revised form, March 21, 2006 Published, JBC Papers in Press, April 6, 2006, DOI 10.1074/jbc.M600205200

Danuta Tomkiewicz[‡], Nico Nouwen[‡], Ruud van Leeuwen[§], Sander Tans[§], and Arnold J. M. Driessen[‡1]

From the [‡]Department of Microbiology, Groningen Biomolecular Sciences and Biotechnology Institute and the Materials Science Centre Plus, University of Groningen, Kerklaan 30, 9751 NN Haren, The Netherlands and [§]Foundation for Fundamental Research on Matter, Institute for Atomic and Molecular Physics, Kruislaan 407, 1098 SJ Amsterdam, The Netherlands

In *Escherichia coli*, secretory proteins (preproteins) are translocated across the cytoplasmic membrane by the Sec system composed of a protein-conducting channel, SecYEG, and an ATP-dependent motor protein, SecA. After binding of the preprotein to SecYEG-bound SecA, cycles of ATP binding and hydrolysis by SecA are thought to drive the stepwise translocation of the preprotein across the membrane. To address how the length of a preprotein substrate affects the SecA-driven translocation process, we constructed derivatives of the precursor of the outer membrane protein A (proOmpA) with 2, 4, 6, and 8 in-tandem repeats of the periplasmic domain. With increasing polypeptide length, an increasing delay in the time before full-length translocation was observed, but the translocation rate expressed as amino acid translocation per minute remained constant. These data indicate that in the ATP-dependent reaction, SecA drives a constant rate of preprotein translocation consistent with a stepping mechanism of translocation.

Translocation of secretory proteins (preproteins) across the cytoplasmic membrane of *Escherichia coli* is mediated by a multisubunit membrane-embedded complex termed "translocase" (1). Translocase consists of a protein-conducting channel, SecYEG, and a peripheral ATPase, SecA. During or shortly after synthesis, the chaperone SecB binds the preprotein, maintains it in a translocation-competent state, and targets it to the SecYEG-bound SecA (2, 3). Subsequently, the preprotein is translocated through the SecYEG pore using the energy from ATP hydrolysis and the proton-motive force (4–6).

In eukaryotes two hypotheses for the translocation of proteins across organellar membranes have been proposed: the "power-stroke" and the "molecular ratchet" mechanism (7–9). In prokaryotes the same mechanisms could drive the translocation of preproteins across the cytoplasmic membrane. In the power-stroke model, SecA would act as a force-generating motor; it binds to the preprotein, pushes it into the channel by binding of ATP, and then releases it in the channel upon the hydrolysis of ATP. Experimental evidence suggests that consecutive unfolded polypeptide segments of ~5 kDa are threaded through the SecYEG pore by cycles of ATP binding and hydrolysis at SecA (10–12). However, it is not clear whether this fixed step size is maintained throughout the translocation reaction. This stepwise translocation model (or power-stroke model) predicts that the time required for the translocation of a preprotein is directly correlated to its length. Likewise, the amount of ATP required for translocation would be a linear function of the preprotein length. On the other hand, different factors may delay or accelerate translocation and the timing of the events. For instance, mildly hydrophobic polypeptide segments cause the accumulation of specific translocation intermediates that are stalled in the translocation pore (13). Such polypeptide segments likely slow down the overall translocation reaction.

The second model, known as molecular ratchet-like (or thermal ratchet/Brownian ratchet) mechanism (9, 14), suggests that the preprotein translocation through the pore is driven by Brownian motion. In this scenario, SecA binding would prevent backsliding of the preprotein into the cytoplasm, thereby providing directionality to the translocation reaction. Consequently, an arrest in the translocation reaction may be followed by hysteresis movements of the polypeptide chain within the translocation pore. This will drive the preprotein back and forth toward an energy minimum that is dictated by favorable interactions between preprotein and SecYEG pore wall and/or folding of the preprotein on either side of the membrane. Indeed, when SecA is physically removed from the SecYEG pore, hysteresis movements of a preprotein translocation intermediate in the translocation channel have been observed (10, 15). The molecular ratchet model therefore predicts that the translocation kinetics are determined mainly by the physicochemical properties (*i.e.* folding characteristics and amino acid composition) of the preprotein. In this model, SecA-mediated translocation steps will be of variable sizes.

Basic questions on the translocation kinetics that may discriminate between the two translocation models have not yet been addressed experimentally. For instance, how does the length of a preprotein substrate affect the kinetics and energetics of translocation? To examine these questions, we have investigated the SecA-mediated translocation kinetics using a quantitative fluorescent assay. To increase the length of a preprotein, we constructed precursor of the outer membrane protein A (proOmpA)[2] derivatives with 2, 4, 6, and 8 in-tandem repeats of the periplasmic domain. This resulted in a large size range of the preprotein from 347 to maximum 1397 amino acids. Quantitative analysis of the translocation kinetics of proOmpA *versus* extended proOmpA variants revealed that the time required to detect full-length translocation depends on the preprotein length and ATP concentration, whereas the rate of amino acid translocation is independent of preprotein length. These data indicate that in the ATP-dependent reaction SecA drives a constant rate of preprotein translocation.

EXPERIMENTAL PROCEDURES

Strains and Materials—Inner membrane vesicles (IMVs) containing overproduced SecYEG were isolated from *E. coli* strain NN100 (SF100, *unc*$^-$) (16) containing plasmid pET605 (17). These membranes lack the entire F_1F_0-ATPase complex and consequently are unable to generate a

* This work was supported by the Foundation for Fundamental Research on Matter, Earth and Life Sciences and the Royal Academy of Sciences of the Netherlands. The costs of publication of this article were defrayed in part by the payment of page charges. This article must therefore be hereby marked "*advertisement*" in accordance with 18 U.S.C. Section 1734 solely to indicate this fact.

[S] The on-line version of this article (available at http://www.jbc.org) contains supplemental Fig. S1.

[1] To whom correspondence should be addressed. Tel.: 31-50-3632164; Fax: 31-50-3632154; E-mail: a.j.m.driessen@rug.nl.

[2] The abbreviations used are: proOmpA, precursor of the outer membrane protein A; IMV, inner membrane vesicle.

Supplemental Material can be found at:
http://www.jbc.org/cgi/content/full/M600205200/DC1

proton-motive force upon addition of ATP. SecA (18) and His-tagged SecB (19) were purified as described previously.

Introduction of Multiple Periplasmic Domains into ProOmpA—Cysteine-less *OmpA* from plasmid pNN208 was cloned into pUC19, resulting in plasmid pEK200. Next, a cysteine codon was introduced at the extreme 5′-end of the *ompA* gene (pEK201) using the QuikChange™ site-directed mutagenesis kit (Stratagene). Subsequently, two unique restriction sites were introduced: (i) a SalI site at the hinge region between the β-barrel and the periplasmic domain, and (ii) a XhoI site just before the cysteine residue at the C terminus (pEK203). The SalI and XhoI restriction sites have compatible cohesive ends that enable the duplication events. To duplicate the periplasmic domain, plasmid pEK203 was digested with EcoRI and XhoI and the fragment encoding *OmpA* without C-terminal cysteine residue was isolated (fragment A). Digestion of plasmid pEK203 with SalI and EcoRI resulted in a fragment encoding the periplasmic domain with the remaining vector (fragment B). Ligation of both fragments (A+B) results in an *ompA* gene with an additional periplasmic domain and a remaining XhoI restriction site that can be used for introduction of additional periplasmic domains. Using the procedure described above, an *ompA* gene with 2, 4, 6, and 8 in-tandem repeats of the periplasmic domain was obtained (pEK206, pEK208, pEK209, and pEK210, respectively). For overproduction of proOmpA (termed proOmpA-P1) and proOmpA derivatives P2, P4, P6, and P8, genes encoding corresponding proteins were cloned (BamHI, HindIII) into expression vector pJF118, giving plasmids pEK204, pEK211, pEK212, pEK213, and pEK214, respectively.

Purification and Labeling of ProOmpA and ProOmpA Derivatives—ProOmpA and proOmpA derivatives were overproduced at 30 °C in strain MM52 (F^-, Δ*lac*U169, *ara*D139, *rps*L, *thi*, *rel*A, *pts*F25, *deo*C1, *sec*A51) (20). After harvesting the cells, inclusion bodies were purified as described (21). ProOmpA and proOmpA-P2, P4, and P6 were further purified using a Q-Sepharose column (Amersham Biosciences). ProOmpA-P8 was purified by gel filtration on a Superose 6HR 10/30 column (Amersham Biosciences) in 50 mM glycine, pH 10.0, 8 M urea, 1 mM dithiothreitol (buffer A). Fractions containing proOmpA-P8 were pooled and concentrated on a Q-Sepharose column (Amersham Biosciences) in buffer A or by the use of Centriprep YM-50 columns (Amicon Bioseparations). After purification, proteins were dialyzed against 50 mM bis-Tris propane, pH 7.4, 6 M urea (buffer B). ProOmpA-P1 and proOmpA derivatives were labeled with fluorescein maleimide (Molecular Probes) as described previously (22). Free label was removed by extensive dialysis against buffer B. Proteins were stored at −80 °C. The labeling efficiency of the proteins was determined using absorbance values at 280 and 490 nm, respectively.

In Vitro Translocation Reactions—*In vitro* translocation of fluorescein-labeled preprotein (22) was assayed as described previously (23). Briefly, reactions were performed in translocation buffer (50 mM Hepes-KOH, pH 7.5, 5 mM $MgCl_2$, 50 mM KCl, 2 mM dithiothreitol, 0.1 mg/ml of bovine serum albumin with 40 μg/ml of SecB, 40 μg/ml of SecA, and 100 nM urea-denatured preprotein (proOmpA-P1 or P2, P4, P6, P8). IMVs containing high SecYEG levels (derived from *E. coli* NN100) were added to a final concentration of 40 μg/ml. Reactions were started by the addition of 1 mM ATP and incubated for various times at 37 °C. Reactions were stopped by chilling on ice. Non-translocated material was degraded by proteinase K treatment (11); thereafter, the translocated material was analyzed by SDS-PAGE followed by direct in gel visualization using a Roche Lumi Imager F1 (Roche Applied Science) (22). Translocation efficiency is expressed as percent of input protein. The time required to detect full-length translocation was determined from gels that have been exposed for 1 s using the fluorescence Imager. To analyze the effect of the ATP concentration on the kinetics of protein translocation, the *in vitro* translocation assay, as described above, was performed with low concentrations of ATP (5–100 μM) in the presence of an ATP regeneration system (10 mM phosphocreatine and 50 μg/ml of creatine kinase).

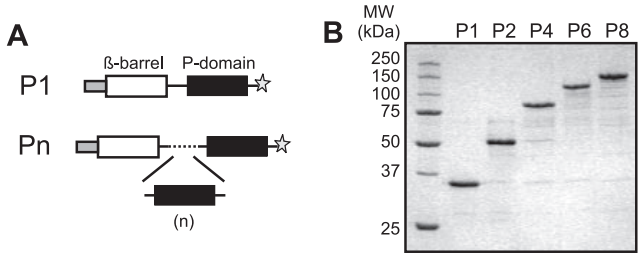

FIGURE 1. **Schematic representation and purification of proOmpA derivatives with in-tandem copies of the periplasmic domain ($n = 1, 3, 5, 7$).** *A*, the signal sequence, β-barrel, and periplasmic domain are indicated by the *gray*, *white*, and *black boxes*, respectively. *Star*, unique C-terminal cysteine residue labeled with fluorescein maleimide. *B*, 5 μg of purified proOmpA-P1, P2, P4, P6, and P8 were separated by 10% SDS-PAGE and stained with Coomassie Brilliant Blue. Positions of molecular mass markers (in kDa) are indicated.

Translocation ATPase Assay—Translocation ATPase activity of the different proOmpA derivatives was determined by taking samples in the linear range of protein translocation and measuring the amount of released free phosphate using the malachite green assay (24). All measurements were done in triplicate, and values were corrected for background ATPase activity.

Other Techniques—Protein concentrations were determined using a DC protein assay kit (Bio-Rad) with bovine serum albumin as a standard.

RESULTS

Construction and Purification of ProOmpA Derivatives with Multiple Copies of the Periplasmic Domain—Previous *in vitro* studies using low concentrations of ATP suggested that SecA-driven protein translocation is a stepwise process with the occurrence of discrete translocation intermediates (11). To examine the SecA-driven translocation reaction at normal ATP levels, we decided to investigate how the length of the preprotein affects the kinetics of translocation. A widely used substrate in *in vitro* protein translocation studies is the precursor of outer membrane protein A (proOmpA). OmpA consist of two domains, an N-terminal hydrophobic β-barrel that is embedded in the outer membrane (25) and a C-terminal domain that is exposed to the periplasm (26). As the C-terminal domain is hydrophilic and clearly separated from the β-barrel domain via a hinge region, this domain was chosen to systematically increase the length of the preprotein. To enable this, unique restriction sites were introduced in the hinge region, which connects the β-barrel with the periplasmic domain, and at the C terminus of the preprotein. This allowed the construction of genes encoding preproteins with multiple in-tandem repeats of the periplasmic domain (residues 194–344) via restriction and ligation (Fig. 1*A*). Compared with the original proOmpA molecule (347 amino acids; P1), a maximum 4-fold increase in length was obtained with the proOmpA derivative containing 8 repeats of the C-terminal domain (1397 amino acids; proOmpA-P8; Table 1). In the construction procedure, a cysteine residue was also introduced at the extreme C terminus of the protein, which enables its unique labeling with the thiol-reactive fluorescent dye fluorescein maleimide. All proOmpA derivatives were highly expressed and could be purified from the SecA-compromised *E. coli* strain MM52 (Fig. 1*B*).

Rate of Amino Acid Translocation Is Independent of the Preprotein Length—To examine how the length of the preprotein affects the SecA-dependent translocation reaction, translocation kinetics of C-terminal fluorescein-labeled proOmpA derivatives were studied by using a pro-

tease protection assay followed by direct fluorescent detection in the gel (22). Quantitative analysis of the labeling efficiency indicated that all proOmpA derivatives were equally labeled with fluorescein maleimide, with an efficiency of ~45%. This ensures a uniform sensitivity of the assay for all proOmpA derivatives. Commonly, translocation reactions are performed with non-saturating preprotein concentrations, *i.e.* radiochemical amounts of preprotein. This precludes a quantitative analysis of translocation as the initial rate will not be at maximal velocity. Therefore, we first examined the effect of preprotein concentration on the translocation rate of the shortest (proOmpA-P1) and longest (P8) precursor proteins. For both precursor proteins the maximal translocation velocity was reached at a precursor protein concentration of 0.1 μM (supplemental Fig. S1). Therefore, this concentration was used in the rest of the translocation experiments. Because of the large size, the resolution of the SDS-PAGE gel was insufficient to detect the processing of proOmpA-P2, P4, P6, and P8 into their respective mature forms, whereas with proOmpA-P1 the precursor and mature forms of the protein are clearly visible. Translocation of all fluorescein-labeled proOmpA derivatives into IMVs was dependent on SecA and SecB and stimulated by the proton-motive force as observed for the wild-type proOmpA (data not shown). As the proton-motive force alone can drive late stages of protein translocation, the presence of this energy source would make it impossible to analyze the effect of the precursor protein length on the SecA-driven translocation reaction. For this reason, all translocation reactions are performed in the absence of a proton-motive force (Fig. 2*A*). All proOmpA derivatives were translocated under those conditions, but clear differences in kinetics were evident. First, as compared with the wild-type protein (proOmpA-P1), longer proOmpA derivatives show an increased delay in time before translocation can be detected (120 and 30 s for proOmpA-P8 and P1, respectively) (Fig. 2*B*). The estimated delay times from three independent experiments were averaged and plotted as a function of the protein length. This revealed a near to linear relationship between the protein length and delay time (Fig. 2*C*). Because all proOmpA derivatives are fluorescently labeled at their extreme C terminus, the results indicate that, for instance, proOmpA-P1 is translocated faster across the membrane as compared with proOmpA-P8. Second, within the linear range of translocation, the translocation rate, expressed as amount of translocated preprotein (in moles) per minute, decreases reverse proportionally with the preprotein length (0.77 and 0.16 pmol/min for proOmpA-P1 and proOmpA-P8, respectively) (Fig. 3*A*). This is consistent with the notion that a longer preprotein requires more time to be fully translocated across the membrane. Interestingly, when we express the translocation rate as the amount of amino acids translocated per minute, the numbers for all proOmpA derivatives are virtually identical (~270 pmol amino acid/min) (Fig. 3*B*). This suggests that all proOmpA derivatives are translocated with similar constant rates.

To investigate the ATP consumption during translocation, we measured the amount of free phosphate released per time unit during the linear range of translocation. The rate of ATP hydrolysis was similar for all proOmpA derivatives (~1.42 nmol free phosphate/min) (Fig. 3*C*). Taking into account that for each of the proOmpA derivatives the rate of translocation as expressed in number of amino acids per time is similar, the coupling efficiency to ATP hydrolysis is also comparable. From these data, it can be calculated that ~5 molecules of ATP are hydrolyzed per translocated amino acid, which suggests a very poor coupling efficiency in these *in vitro* experiments.

SecA Motor Function Determines the Kinetics of Translocation—Our data indicate that the preprotein translocation rate, expressed as amino acid translocated/time interval, is independent of the length of the preprotein. To further examine the SecA motor activity, the influence of the ATP concentration on the translocation kinetics was determined. Reducing the ATP concentration below 20 μM leads to a drastic reduction in the translocation rate of proOmpA-P1 (Fig. 4*B*) and a significant increase in the delay in time before full-length translocation is detectable (Fig. 4, *A* and *C*). Similar observations were made for the longest

TABLE 1
Molecular characteristics of proOmpA derivatives with multiple copies of the periplasmic domain

ProOmpA derivative	Number of periplasmic domains	Number of amino acids	Mass
			kDa
P1	1	347	37.3
P2	2	497	53.3
P4	4	797	85.4
P6	6	1097	117.4
P8	8	1397	149.4

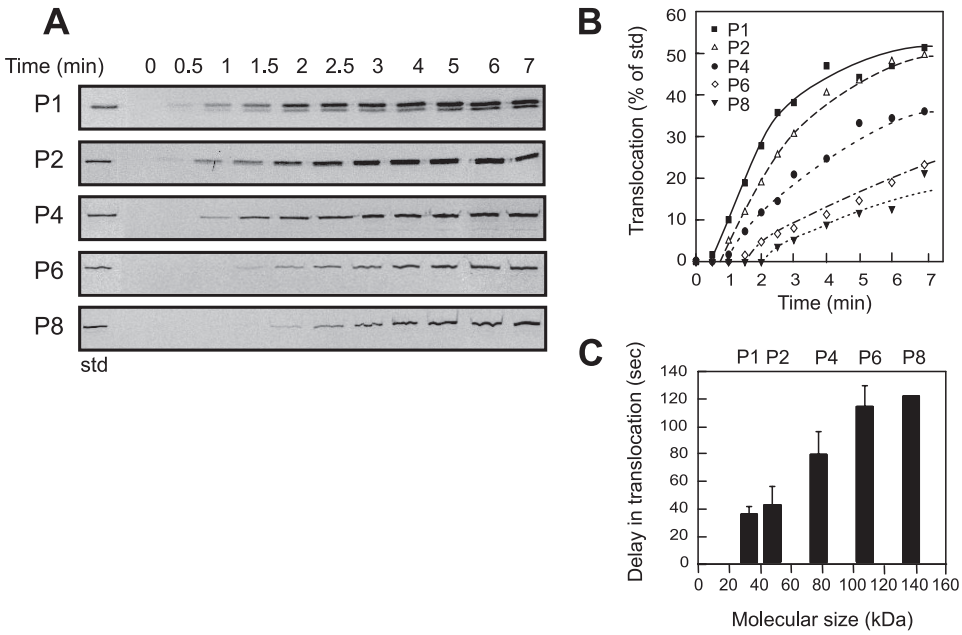

FIGURE 2. **Translocation kinetics of proOmpA derivates with multiple copies of the periplasmic domain.** *A*, translocation of proOmpA-P1, P2, P4, P6, and P8 into IMVs derived from *E. coli* strain NN100 in the absence of a proton-motive force. Reactions were carried out as described under "Experimental Procedures." *std*, 10% of the input material. *B*, quantification of results shown in *panel A*. ProOmpA-P1 (*black squares/solid line*), proOmpA-P2 (*white triangles/dashed line*), proOmpA-P4 (*black circles/small dashed line*), proOmpA-P6 (*white diamonds/dash-dot line*), and proOmpA-P8 (*black upside-down triangles/dotted line*). *C*, experiments shown in *panel A* were used to determine the time required to detect full-length translocation. To obtain more accurate data for proOmpA-P1 and P2, experiments were performed using shorter times of translocation. Data are an average of at least three independent experiments.

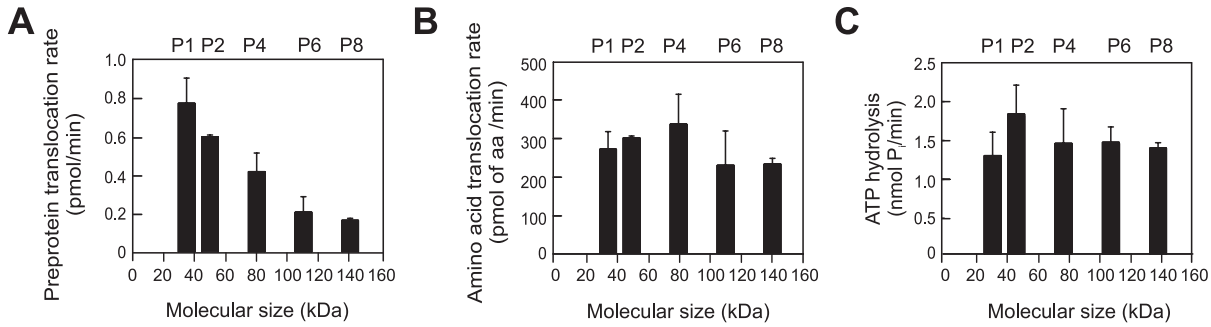

FIGURE 3. **Translocation rate and ATP hydrolysis of proOmpA derivatives with multiple copies of the periplasmic domain.** Experiments shown in Fig. 2 were used to determine the initial rate of translocation of the different proOmpA derivatives and used to calculate the initial rate expressed as amount of translocated preprotein (in pmol) per minute (*A*) or amount of amino acids (in pmol) per minute (*B*). *C*, translocation ATPase activity of the different proOmpA derivatives. ProOmpA derivatives were translocated into IMVs from *E. coli* strain NN100 as described in Fig. 2, and the amount of released inorganic phosphate was determined during the linear range of translocation. All data are an average of at least three independent experiments.

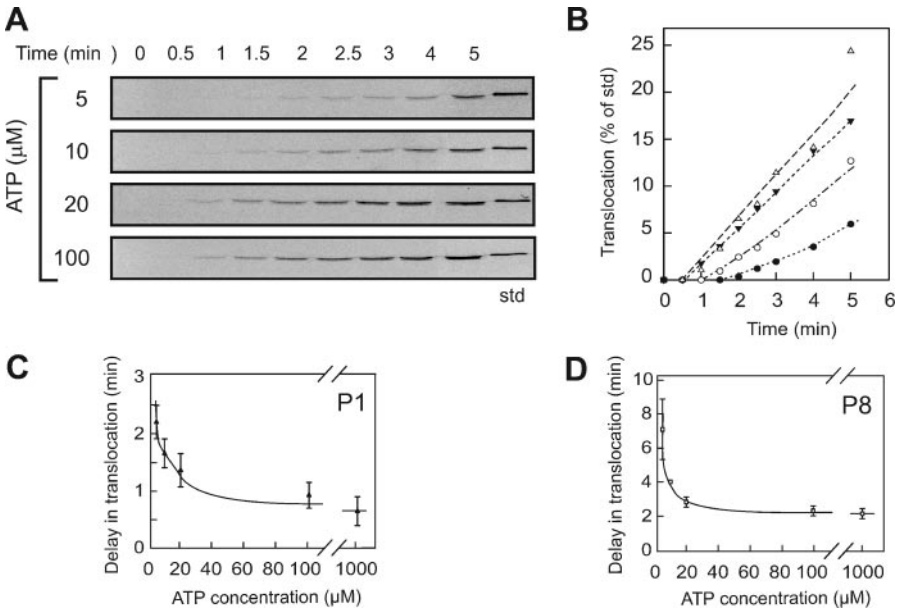

FIGURE 4. **Translocation kinetics at different ATP concentrations.** *A*, ProOmpA-P1 translocation into IMVs from *E. coli* NN100 cells at different ATP concentrations (5–100 μM). *B*, quantification of results shown in *panel A*. ATP concentrations shown are 100 μM (*white triangles/dashed line*), 20 μM (*black upside-down triangles/small dashed line*), 10 μM (*white circles/dash-dot line*), and 5 μM (*black circles/dotted line*). Translocation time required to detect full-length translocation in relation to the ATP concentration for proOmpA-P1 (*P1*) (*C*) and proOmpA-P8 (*P8*) (*D*). Data are an average of at least three independent experiments.

preprotein, proOmpA-P8 (Fig. 4*D*). From these data, an apparent K_m for ATP for translocation can be calculated of ~12–18 μM. These results demonstrate that the delay in full-length translocation for longer preproteins (see Fig. 2) is dependent on the SecA motor function. Taken together, the results demonstrate that the rate of protein translocation is controlled by the ATP concentration and independent from the length of the preprotein.

DISCUSSION

In recent years, our understanding of the structure and function of components of the bacterial secretion machinery has increased considerably. However, the mechanism of energy coupling to preprotein translocation is only poorly understood. In addition, the kinetics of translocation has barely been studied quantitatively. ATP is an essential energy source, and a key question concerns how ATP is utilized by SecA to drive translocation: Does SecA function as a uni-directional stepping motor that "pushes" the preprotein through the SecYEG channel, or does translocation proceed according to a molecular ratchet mechanism? In the latter mechanism, translocation would be driven by protein folding at the *trans*-side of the membrane while directionality to the process is provided by SecA, for instance by affecting unfolding at the *cis*-side and/or by preventing backsliding of the preprotein. An *in vitro* translocation assay employing proOmpA as substrate showed that the translocation reaction at low ATP concentration occurs through a number of intermediate steps (10–12). These experiments suggested that SecA is a stepping motor and that a full cycle of ATP binding and hydrolysis results in the translocation of ~50 amino acids. Mechanistically, each step could be subdivided into two distinct translocation events of ~25 amino acids, *i.e.* one elicited by the binding of SecA to the preprotein translocation intermediate and one driven by binding of ATP to SecA (11). On the other hand, hydrolysis of ATP is thought to drive the release of the preprotein from its association with SecA (10–12). It is, however, important to note that discrete proOmpA translocation intermediates have been observed only at low ATP concentration or when translocation is blocked by the addition of non-hydrolyzable ATP analogues. It is also not known if a fixed step size is used throughout the translocation reaction. The possibility remains that other factors contribute to the efficiency of the translocation reaction, such as folding at the *cis*- and *trans*-sides of the membrane (15) or, for instance, interactions of the preprotein with the SecYEG pore wall. Finally, discrete translocation intermediates have not been reported for other preproteins. Therefore, the length and composition of the polypeptide chain may influence the phenomenological step size of protein translocation.

We have analyzed the kinetics and energetics of the translocation of proOmpA derivatives, the length of which has been systematically increased by adding up to 8 in-tandem domains with a similar amino acid composition at the C terminus of proOmpA. As repeating unit we have chosen the periplasmic domain of OmpA because this region is

polar and clearly distinct from the membrane-embedded β-barrel domain, which constitutes about half the length of the wild-type proOmpA. SecB preferentially binds the N-terminal β-barrel domain of proOmpA (28). In agreement with this, we observed that the aggregation of all proOmpA derivatives was effectively suppressed by a stoichiometric amount of SecB (data not shown). We noted that an increase in the length of the preprotein resulted in a progressive increase in the delay time before full-length translocation could be detected (30 s to up to 2 min for proOmpA and proOmpA-P8, respectively). From the linear range of the preprotein translocation reaction, an inverse relation was observed between the length of the preprotein and the translocation rate (from 0.77 pmol/min for proOmpA down to 0.16 pmol/min for P8 protein) (Fig. 3*A*). Importantly, both the delay in time before full-length translocation is detectable and the linear rate of preprotein translocation are dependent on the ATP concentration (Fig. 4). This indicates that the observed effects are directly related to the SecA motor function. When we calculate the translocation rate expressed per translocated amino acid, similar values within the error range are obtained for proOmpA and proOmpA derivatives, *i.e.* ~270 amino acids/minute (Fig. 3*B*). Likewise, the calculated amount of ATP hydrolyzed per translocated amino acid, in the linear range of preprotein translocation, is similar for all preproteins (5 mol^{ATP}/translocated amino acid or 250 mol ATP/50 amino acids). These experimentally determined numbers are very high and more than expected for a translocation progress of ~50 amino acids per turnover of SecA (10, 11). Those high energetic costs are possibly due to a fraction of proOmpA molecules that become jammed in the translocase, giving rise to an excessive ATP hydrolysis. At this stage, the poor coupling efficiency appears to be a general shortcoming/limitation of the *E. coli in vitro* assay (27) rather than a reflection of a mechanistic requirement. For instance, for the translocation of the precursor of maltose-binding protein the ATP requirement seems much lower than observed for proOmpA.

The conditions employed in the *in vitro* assays represent multiple turnovers of the translocase (22). The experimental data show that 4 molecules of proOmpA-P1 (in a total of 1388 amino acids) are translocated in the same time as 1 molecule of proOmpA-P8 (in a total of 1397 amino acids). This implies that, at least *in vitro*, processes such as protein targeting and initiation of translocation are only minor contributors to the total time required to translocate these proteins into the membrane vesicles. Moreover, these data strongly suggest that the actual translocation process is rate determining.

The current data are consistent with a mechanism in which translocation occurs in discrete steps wherein each turnover of SecA results in the translocation progress of a fixed length of the preprotein. Therefore, this study has provided independent support for a stepping mechanism of translocation. However, it should be noted that the data do not discriminate between a power-stroke or molecular ratchet mechanism *per se*. Translocation may be a combination of both mechanisms. For instance, the ATP-dependent SecA-mediated power-stroke may not be employed to actually push the preprotein across the membrane but instead may cause the opening of the translocation channel that allows the diffusion of a fixed preprotein polypeptide length. To obtain a more precise estimate on the stepping mechanism, single molecule studies on translocation events are required.

Acknowledgment—We thank W. K. Smits for helpful discussions.

REFERENCES

1. Wickner, W., Driessen, A. J. M., and Hartl, F. U. (1991) *Annu. Rev. Biochem.* **60,** 101–124
2. Fekkes, P., and Driessen, A. J. M. (1999) *Microbiol. Mol. Biol. Rev.* **63,** 161–173
3. Topping, T. B., and Randall, L. L. (1997) *J. Biol. Chem.* **272,** 19314–19318
4. Chen, L., and Tai, P. C. (1985) *Proc. Natl. Acad. Sci. U. S. A.* **82,** 4384–4388
5. Shiozuka, K., Tani, K., Mizushima, S., and Tokuda, H. (1990) *J. Biol. Chem.* **265,** 18843–18847
6. Yamane, K., Ichihara, S., and Mizushima, S. (1987) *J. Biol. Chem.* **262,** 2358–2362
7. Neupert, W., and Brunner, M. (2002) *Nat. Rev. Mol. Cell. Biol.* **3,** 555–565
8. Matlack, K. E., Misselwitz, B., Plath, K., and Rapoport, T. A. (1999) *Cell* **97,** 553–564
9. Simon, S. M., Peskin, C. S., and Oster, G. F. (1992) *Proc. Natl. Acad. Sci. U. S. A.* **89,** 3770–3774
10. Schiebel, E., Driessen, A. J. M., Hartl, F. U., and Wickner, W. (1991) *Cell* **64,** 927–939
11. van der Wolk, J. P., de Wit, J. G., and Driessen, A. J. M. (1997) *EMBO J.* **16,** 7297–7304
12. Uchida, K., Mori, H., and Mizushima, S. (1995) *J. Biol. Chem.* **270,** 30862–30868
13. Sato, K., Mori, H., Yoshida, M., Tagaya, M., and Mizushima, S. (1997) *J. Biol. Chem.* **272,** 5880–5886
14. Alder, N. N., and Theg, S. M. (2003) *Cell* **112,** 231–242
15. Arkowitz, R. A., Joly, J. C., and Wickner, W. (1993) *EMBO J.* **12,** 243–253
16. Nouwen, N., van der Laan, M., and Driessen, A. J. M. (2001) *FEBS Lett.* **508,** 103–106
17. Kaufmann, A., Manting, E. H., Veenendaal, A. K., Driessen, A. J. M., and van der Does, C. (1999) *Biochemistry* **38,** 9115–9125
18. Cabelli, R. J., Chen, L., Tai, P. C., and Oliver, D. B. (1988) *Cell* **55,** 683–692
19. Fekkes, P., de Wit, J. G., van der Wolk, J. P., Kimsey, H. H., Kumamoto, C. A., and Driessen, A. J. M (1998) *Mol. Microbiol.* **29,** 1179–1190
20. Oliver, D. B., and Beckwith, J. (1981) *Cell* **25,** 765–772
21. Crooke, E., Brundage, L., Rice, M., and Wickner, W. (1988) *EMBO J.* **7,** 1831–1835
22. de Keyzer, J., van der Does, C., and Driessen, A. J. M. (2002) *J. Biol. Chem.* **277,** 46059–46065
23. Cunningham, K., Lill, R., Crooke, E., Rice, M., Moore, K., Wickner, W., and Oliver, D. (1989) *EMBO J.* **8,** 955–959
24. Lill, R., Cunningham, K., Brundage, L. A., Ito, K., Oliver, D., and Wickner, W. (1989) *EMBO J.* **8,** 961–966
25. Pautsch, A., and Schulz, G. E. (1998) *Nat. Struct. Biol.* **5,** 1013–1017
26. Ried, G., Koebnik, R., Hindennach, I., Mutschler, B., and Henning, U. (1994) *Mol. Gen. Genet.* **243,** 127–135
27. Driessen, A. J. M. (1992) *EMBO J.* **11,** 847–853
28. MacIntyre, S., Mutschler, B., and Henning, U. (1991) *Mol. Gen. Genet.* **227,** 224–228

SUPPLEMENTARY MATERIALS

MATERIALS AND METHODS

Effect of the protein concentration on the initial rate of translocation
To analyse the effect of the preprotein concentration on the initial rate of translocation, an *in vitro* translocation assay was performed with different concentrations of preprotein (0.5 – 0.01 μM).

FIGURE LEGEND

Fig. S1. Initial rate of translocation rate as function of the preprotein concentration. Translocation of proOmpA-P1 and P8 into IMV's derived from strain NN100 in the absence of PMF, was performed as described in Materials and Methods.

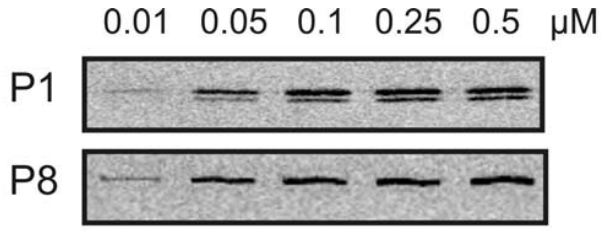

Fig. S1. Tomkiewicz *et al*.